FULL TITLE
ASP Conference Series, Vol. **VOLUME**, **YEAR OF PUBLICATION**
NAMES OF EDITORS

Historic mass loss from the RS Ophiuchi system

Jacco Th. van Loon

Lennard-Jones Laboratories, Keele University, Staffordshire ST5 5BG, United Kingdom; jacco@astro.keele.ac.uk, www.astro.keele.ac.uk/∼jacco

Abstract. Dust has been detected in the recurrent nova RS Ophiuchi on several occassions. I model the historical mid-infrared photometry and a recent Spitzer Space Telescope spectrum taken only half a year after the 2006 eruption. The dust envelope is little affected by the eruptions. I show evidence that the eruptions and possibly the red giant wind of RS Oph may sculpt the interstellar medium, and show similar evidence for the recurrent dwarf nova T Pyxidis.

1. Dusty stellar winds

1.1. Asymptotic Giant Branch stars and red supergiants

Stars with an initial mass between ~ 1 and ~ 40 $M_\odot$ become hydrogen/helium-shell-burning Asymptotic Giant Branch (AGB) stars or core-helium-burning red supergiants (RSG). These phases are characterised by cool, molecular atmospheres giving rise to M spectral types (S or C for some chemically peculiar AGB stars), strong radial pulsations of this atmosphere on timescales of a year or more, and a high luminosity ($L > 2,000$ $L_\odot$). The pulsation may lift the atmosphere high enough such that dust can condense (Bowen & Willson 1991). Radiation pressure on the grains then drives a dust wind which, via collisions with molecular hydrogen, drags the gas along with it. At a typical wind speed $v_\infty \sim 5$ to 30 km s^{-1} these stars lose mass at rates from $\dot{M} \sim 10^{-7}$ to over 10^{-4} $M_\odot$ yr^{-1} (van Loon et al. 1999). In AGB stars this leads to the removal of the mantle and the premature death of the star, leaving the truncated core behind as a cooling white dwarf. The more massive RSGs either explode or evolve back to higher surface temperatures, and it is not yet clear how much mass they will have shed during the preceding RSG stage.

Mass-loss rates of cool, luminous stars are most easily estimated from the reprocessed radiation emitted by the dust grains at infrared (IR) wavelengths, which is particularly conspicuous in the $\lambda \sim 10$ to 40 μm region. The main problem with this method is that the dust constitutes only a minor fraction of the total mass in the wind, typically $\sim$ 1:200 (Knapp 1985) but poorly known for all but the dustiest stars. Carbon monoxide has strong rotational transitions at mm wavelengths which can be detected in relatively nearby stars, but despite being the most abundant molecule after H_2 this too is a trace species of which the mass fraction is uncertain — and modelling the CO line requires knowledge of the temperature profile throughout the envelope which depends, amongst other things, on the dust content.

1.2. First ascent Red Giant Branch stars

Low-mass stars ($M_{\rm initial} < 2$ M$_\odot$) evolve along a first ascent Red Giant Branch (RGB) as hydrogen-shell burning stars with an inert helium core. They reach a maximum luminosity of only $L_{\rm tip} \sim 2,000$ L$_\odot$, and it becomes problematic for them to drive a wind. The situation is worsened by the fact that many RGB stars do not pulsate strongly and slowly enough to sufficiently increase the scaleheight, and the dust condensation is therefore unlikely to reach completeness. With a low, uncertain dust:gas mass ratio and possibly higher dilution of the dust envelope as it kinematically decouples from the bulk gas, measured mass-loss rates will tend to be too low. The threshold below which this happens is not well known, partly because of uncertainties in the opacity of the grains as they nucleate and grow: Gail & Sedlmayr (1987) estimate $\dot{M} \gg 10^{-6}$ M$_\odot$ yr^{-1} but Netzer & Elitzur (1993) place it at $\dot{M} > 10^{-7}$ M$_\odot$ yr^{-1}. Judge & Stencel (1991) show that RGB mass loss must be driven by another mechanism, but that this appears to be similarly efficient as a dust-driven wind. The warmer stars further down the RGB have more prominent chromospheres, which may be accompanied by the generation of Alfvén or acoustic waves that provide a possible alternative mechanism for driving a wind.

Mass-loss rates estimated from the IR emission for the brightest, dustiest RGB stars are typically $\dot{M} \sim 10^{-7}$ to 10^{-6} M$_\odot$ (van Loon et al. 2006; Origlia et al. 2007). Mass-loss rates from $\dot{M} \sim 10^{-9}$ to 10^{-6} M$_\odot$ yr^{-1} have been determined from the blue-displaced cores of strong optical absorption lines and emission in some of these lines, but these are very uncertain too because of the sensitivity to the precise excitation and ionization conditions in the wind. For the most luminous RGB stars the IR and optical estimates tend to agree within an order of magnitude (McDonald & van Loon 2007).

2. The dusty stellar wind of RS Ophiuchi

RS Ophiuchi has a spectral type of M2 (Fekel et al. 2000), and I will later show that the luminosity is $L \sim 444$ L$_\odot$. This places it on an isochrone of a star with an initial mass of $M_{\rm initial} \sim 1.1 \pm 0.1$ M$_\odot$ (Fig. 1). Although it is a few times fainter than the tip-RGB luminosity and not as cool as it gets, mass loss is expected at a level of $\dot{M} > 10^{-9}$ M$_\odot$ yr^{-1} and may be accompanied by dust.

2.1. Mid-IR observations

RS Oph is usually classified as an S-type system, which by definition is a system devoid of dust as the dusty systems are classified as D-type. The latter usually contain a Mira-type large-amplitude variable donor star, which is likely to be an AGB star. RS Oph is not a Mira-type variable, and definitely on the RGB, but it does have circumstellar dust, and the S-type classification is thus misleading. Its IR emission at $\lambda = 10$ μm was detected and attributed to dust for the first time in 1970 by Geisel et al. (1970), which lead them to remark: "The infrared emission from novae closely resembles that from many infrared stars in which the rate of mass loss is more constant. This suggests that the formation of grains is governed by similar processes in all these systems, and that novae are key objects in understanding how the dust is formed."

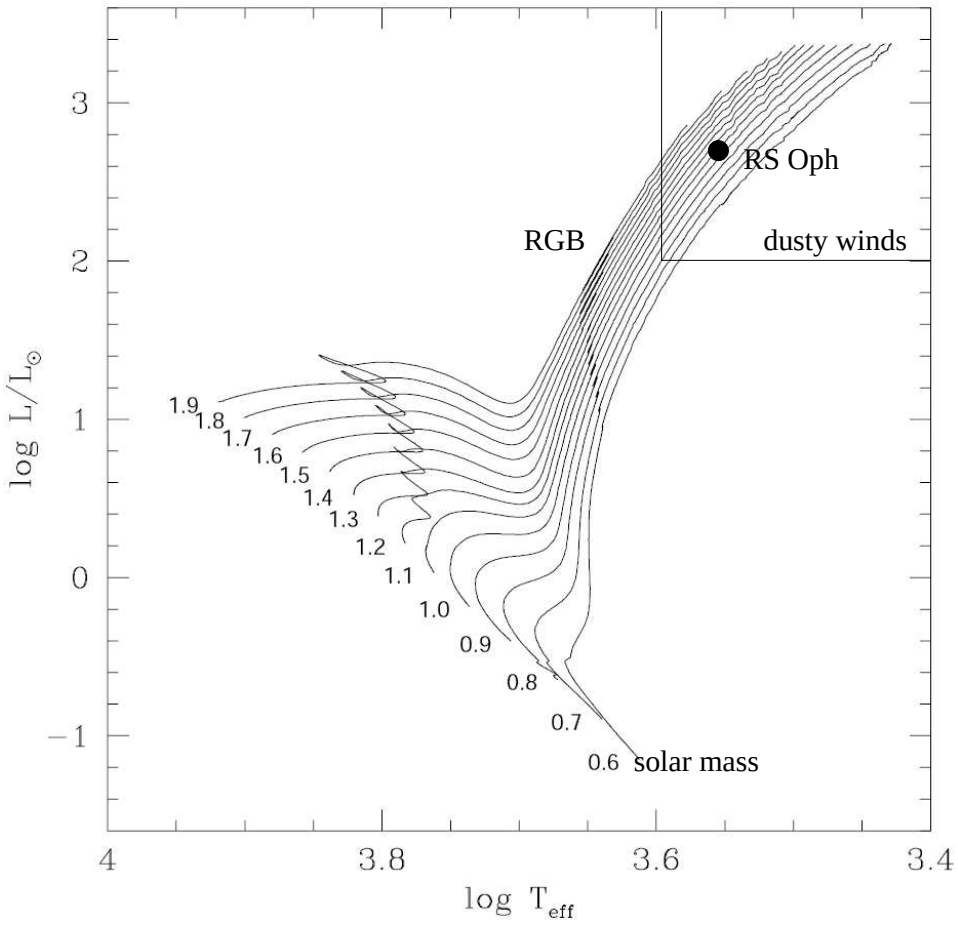

Figure 1. RS Oph compared to isochrones from Girardi et al. (2000).

Dust had thus been detected within three years from the eruption in 1967. RS Oph underwent two more eruptions, in 1985 and in 2006, and as far as I know the system has been observed at mid-IR wavelengths twice more during quiescence and again shortly after the 2006 eruption (Fig. 2). Large differences in the mid-IR emission might be expected depending on the temporal proximity of an eruption, so it came as a surprise to find the contrary.

RS Oph was detected in the InfraRed Astronomical Satellite (IRAS) survey in 1983 (Schaefer 1986). It is listed in the IRAS Point Source Catalogue with

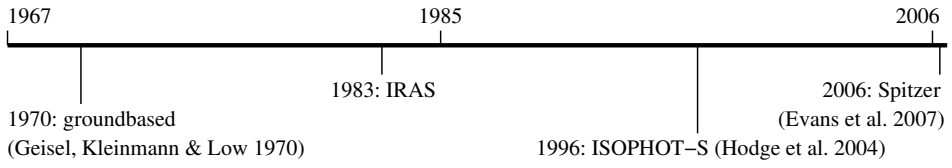

Figure 2. Times of eruptions and mid-infrared observations.

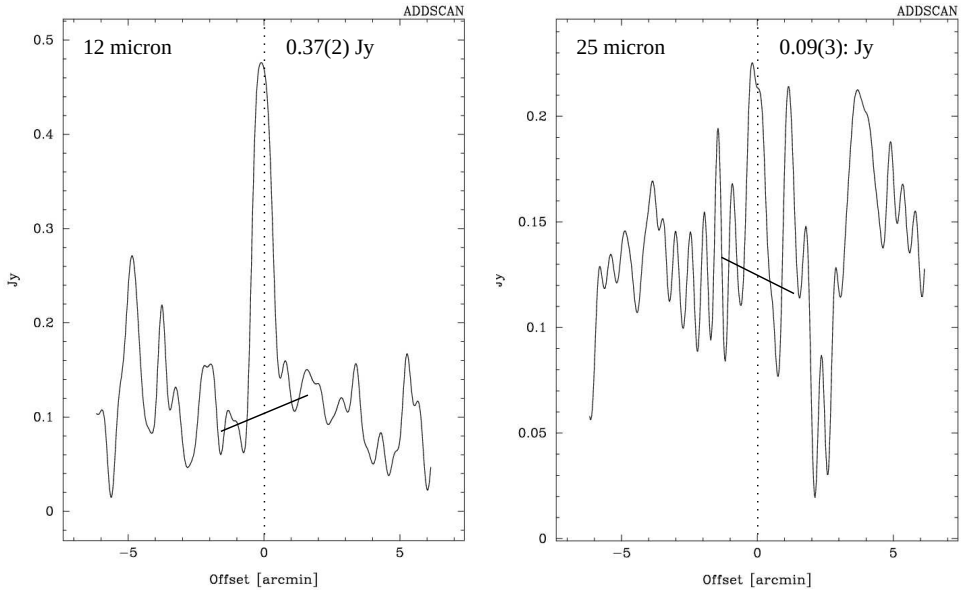

Figure 3. IRAS scans through RS Oph at 12 μm (left) and 25 μm (right).

$F_{12} = 0.4$ Jy and $F_{25} < 0.32$ Jy (the upper limits at 60 and 100 μm are meaningless); Kenyon, Fernandez-Castro, & Stencel (1988) estimate $F_{12} = 0.38$ Jy and $F_{25} = 0.12$ Jy, and Harrison & Gehrz (1994) estimate $F_{12} = 0.41 \pm 0.04$ Jy and $F_{25} = 0.14 \pm 0.04$ Jy. I have re-measured the IRAS scans, and derive refined estimates of $F_{12} = 0.37 \pm 0.02$ Jy and $F_{25} = 0.09{:}\pm 0.03$ Jy (Fig. 3). Kenyon, Fernandez-Castro, & Stencel (1986) estimated $F_{12} = 0.30$ Jy and $F_{25} = 0.16$ Jy from pointed observations carried out with IRAS in September 1983 (they estimate that free-free emission may contribute ~ 0.03 and ~ 0.04 Jy at $\lambda = 12$ and 25 μm, respectively). The IRAS 12-μm flux densities are in remarkably good agreement with the Geisel et al. (1970) measurement of $F_{10.4} \sim 0.4$ Jy (an N-band magnitude of $m_{\rm N} \sim 4.5$ to 5.1 mag) a dozen years earlier. Then again, there had not been any eruption meanwhile.

Soon after the end of the IRAS mission, RS Oph put up a show again. Curiously, it took more than a decade until new mid-IR measurements were made, in March 1996 with the PHOT-S instrument onboard the Infrared Space Observatory (ISO). Hodge et al. (2004) analysed the spectrum shortward of $\lambda = 9$ μm and found no evidence for dust emission. However, at those wavelengths the dust emission is < 0.1 Jy; the uncertainties in zodiacal light correction and instrument calibration and sensitivity do not permit the detection of the dust emission in the PHOT-S spectrum around 8-11 μm.

Another decade passed before new mid-IR measurements were made, this time with the Spitzer Space Telescope (Spitzer) triggered by the February 2006 eruption. By September 2006 the free-free and line emission had weakened enough to reveal a continuum and spectral features unambiguously identifiable with predominantly silicate-type dust (Evans et al. 2007). Remarkably, the Spitzer spectrum agrees frightfully well with all previous photometry (Fig. 4).

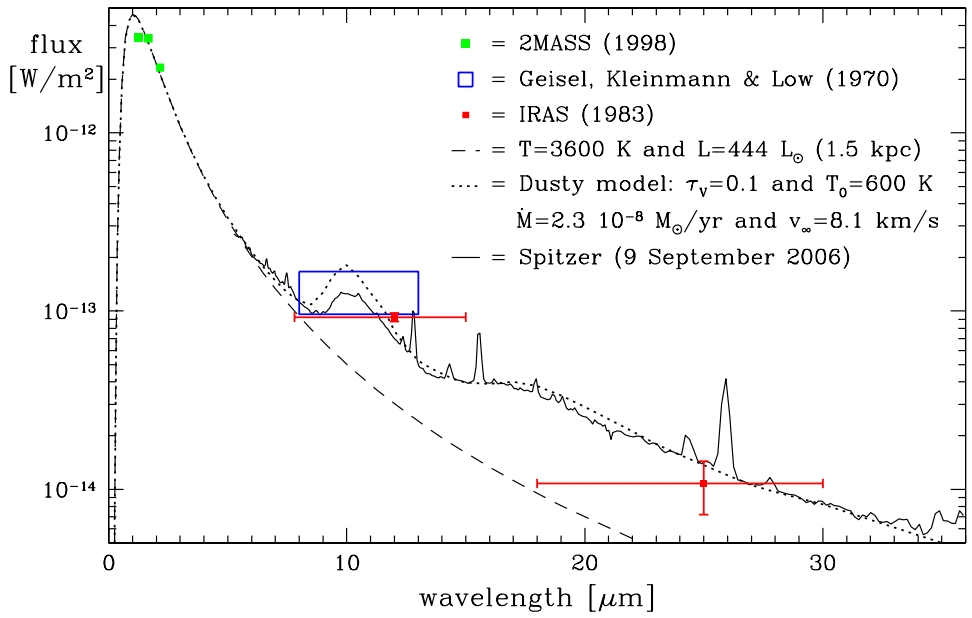

Figure 4. Photometry and Spitzer spectrum, overlain with a black body representing the star and a Dusty model that reproduces the envelope.

2.2. Modelling the dust envelope

I used the radiative transfer code Dusty (Ivezić & Elitzur 1997) to model the spectral energy distribution (SED). The main input parameter of interest is the optical depth, $\tau_{\rm V}$, which is related to the mass-loss rate via the dust:gas mass ratio (assumed to be 1:200), luminosity ($L = 444$ L$_\odot$, measured from the fit to the data assuming a distance of 1.5 kpc) and wind speed (computed by the model for a dust-driven wind). The second input parameter of interest is the temperature at the inner edge of the dust envelope, T$_0$. The model SED also depends on the dust species used, and on the temperature of the star (for which we adopt $T = 3,600$ K consistent with its spectral type). A good fit was obtained using circumstellar silicates from Ossenkopf, Henning, & Mathis (1992), and $T_0 = 600$ K. The model overestimates the strength of the 10-μm feature, but this also depends on the grain properties such as size, shape and composition (a (Mathis, Rumpl, & Nordsieck 1977) size distribution was assumed).

I thus estimate a mass-loss rate $\dot{M} = 2.3 \times 10^{-8}$ M$_\odot$ yr^{-1} at a wind speed $v_\infty = 8.1$ km s^{-1}. Although silicates can form already at temperatures above 1,000 K there is a conspicuous absence of such warm dust ($T > 600$ K). Because the dust shell is optically thin the SED does not depend much on the geometry. Assuming a spherically symmetric wind, the dust envelope starts at a distance of 39 R$_\star$ (~ 10 AU) from the red giant (the outer radius is not constrained by the available data other than that it is $\gg 10^2$ R$_\star$); the orbital radius is ~ 1 AU (Fig. 5). Although the wind is unlikely to travel at a constant speed v_∞ before dust even forms, it would take 6 years to reach the dust formation zone if it did; the binary would have gone round nearly five times and it is thus highly unlikely that the binary motion leaves non-axisymmetric imprints on the dust shell.

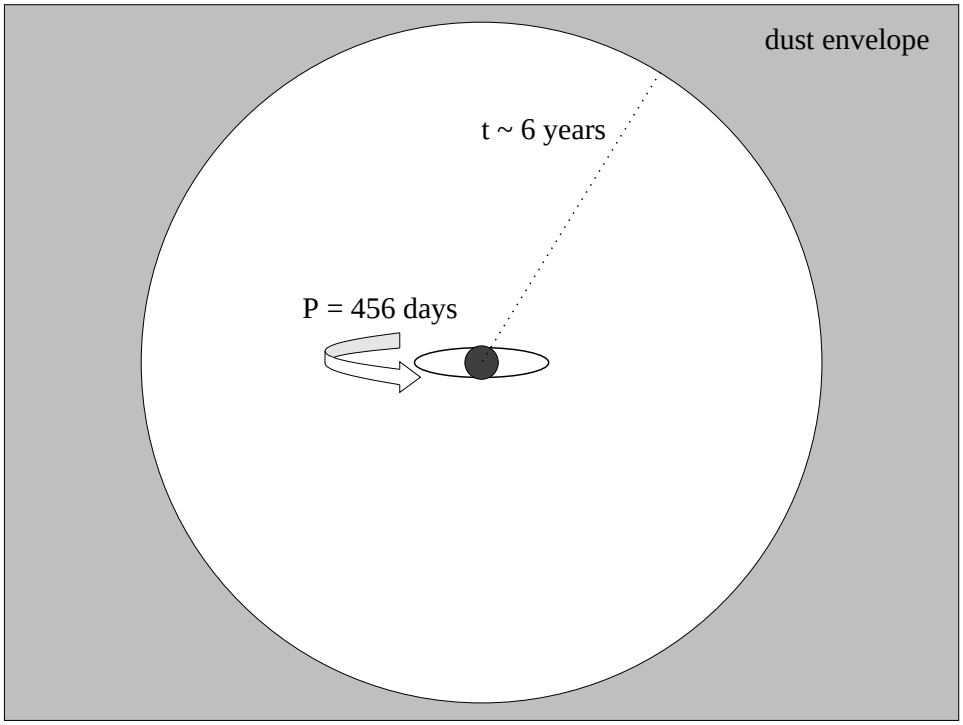

Figure 5. Sketch of the geometry of the RS Oph system, roughly to scale.

2.3. How typical is the mass-loss rate of RS Oph?

It has been suggested that symbiotic stars lose mass more rapidly than single stars (Kenyon 1988). However, when comparing RS Oph with other dusty stars I find no evidence for a particularly high mass-loss rate. In Fig. 6 the differences are plotted between the measured mass-loss rate and the one predicted by the formula for dust-driven winds of oxygen-rich AGB stars and RSGs (van Loon et al. 2005). RS Oph sits at the warm end of the diagram, where many stars appear to have lower mass-loss rates or a lower dust content (including the famous RSGs Betelgeuse and μ Cep). Yet its mass-loss rate is nearly as expected for a well-developed, efficiently dust-driven wind. Although at the faint end of the distribution, RS Oph is also in line with what is measured for red giants in globular clusters (McDonald & van Loon 2007, their Fig. 13).

On the other hand, stars that do not pulsate in the fundamental mode, like Miras do, have lower mass-loss rates or less complete dust formation (Fig. 6). Compared to those cooler stars, RS Oph seems to have a rather high mass-loss rate. The mass-loss rate of RS Oph may even have been under-estimated, if the dust:gas ratio is lower than assumed. Physical mechanisms exist that might explain enhanced mass loss in symbiotic systems, e.g., through equatorial collimation or tides (Mikołajewska 2000).

The remarkable observation is that the system has been losing mass at a (near) constant rate, and that the eruptions have done little to affect the dust envelope. This can be understood if the eruptions are highly an-isotropic.

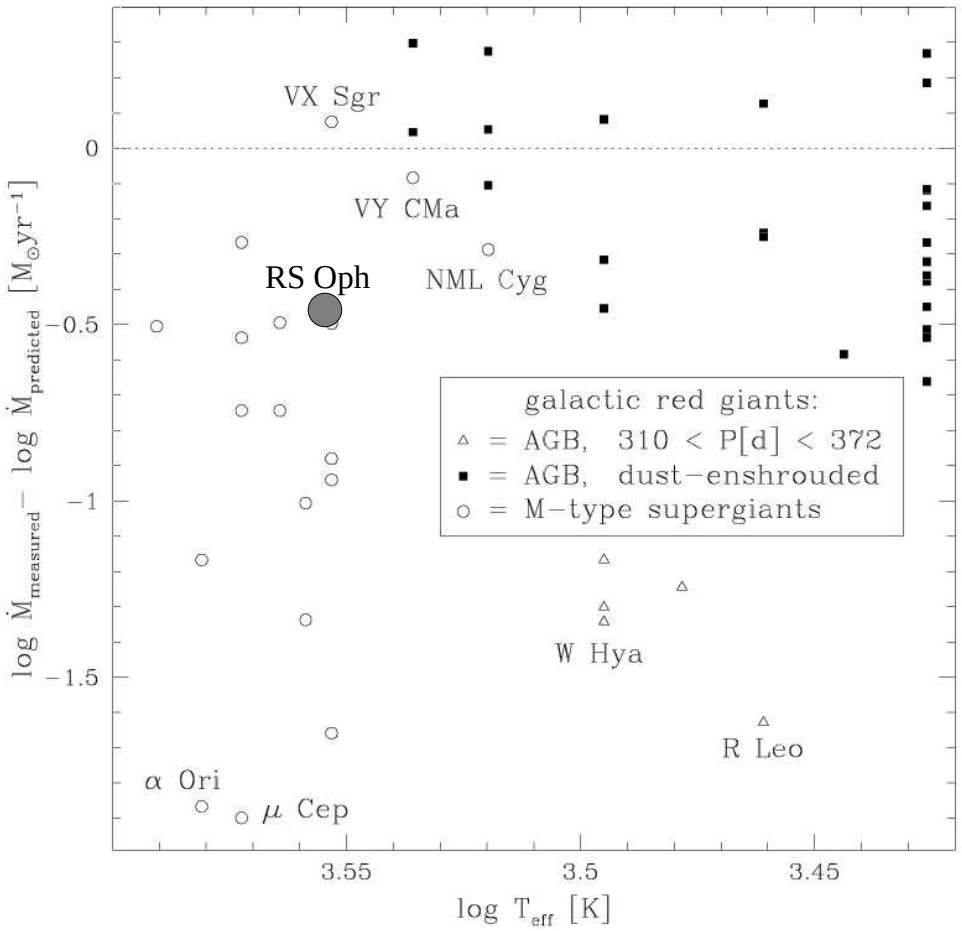

Figure 6. RS Oph compared with other dusty red giants, and with predictions.

3. Do recurrent novae affect the interstellar medium?

Recurrent novae are relatively old systems, and hence they have developed large peculiar velocities with respect to the ISM. It is therefore possible that recurrent novae carve out a path through the ISM as their winds sweep up ISM material and/or the nova eruptions leave a trail of successive shells.

3.1. The case of RS Oph

A composite of IRAS images at 12, 25 and 60 μm reveals a dark patch of 1-2° diameter around RS Oph (Fig. 7) — the direction of the galactic plane is towards the lower-left corner. After scaling to the same mean and spread, a median combination of all 12-100 μm images shows an elongated cut into the ISM, with RS Oph near its end and its proper motion pointing at a trajectory along it. In the same time it took RS Oph to traverse along the structure ($\sim$ 1 Myr), its wind would have blown a bubble of $\sim$ 1° diameter (Fig. 7). This is highly suggestive of RS Oph being responsible for the ISM structure.

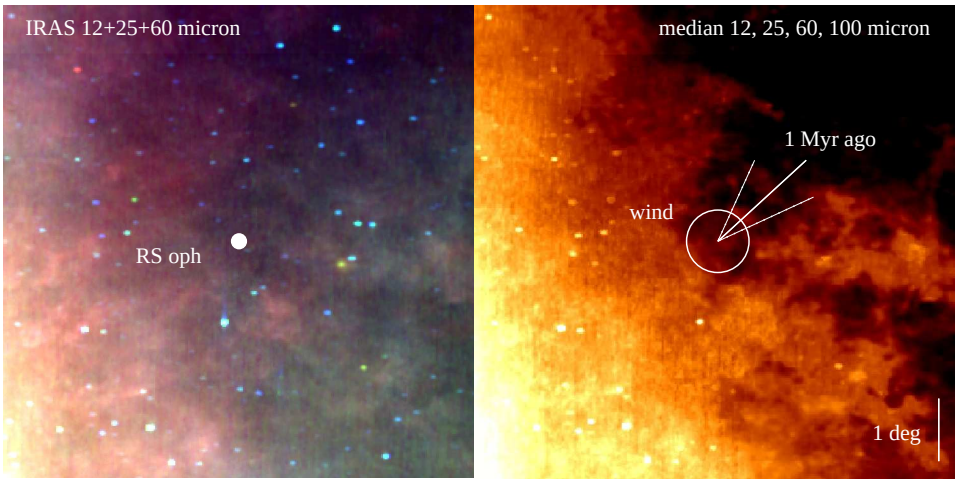

Figure 7. IRAS composites around RS Oph (North is up, East is left); the right panel is a median combination of scaled 12, 25, 60 and 100 μm images.

An Hα map (Finkbeiner 2003) shows what looks like a bubble of ionized gas, with RS Oph near its western edge (Fig. 8). Cool et al. (2005) noticed this structure when studying the nearby symbiotic binary XX Oph; they estimate a radial velocity of $v = 2.4 \pm 11.8$ km s^{-1} for the gas and exclude an association with XX Oph. RS Oph has $v = -40$ km s^{-1} (Fekel et al. 2000) and is therefore also not associated with the extended Hα emission. However, combined with the dust map from Schlegel, Finkbeiner, & Davis (1998) the ISM structure more closely resembles a hole in the dust through which background emission is seen, rather than a hot bubble (Fig. 8). Composed of a Be star and a late-M giant, XX Oph rather than RS Oph might have created the ISM structure.

3.2. The case of T Pyx

IRAS images around the recurrent dwarf nova T Pyxidis (Gilmozzi & Selvelli 2007, and references therein) also show a cavity, with a 2$''$ diameter (Fig. 9). A 10$''$ diameter hot shell was linked with the 1944 eruption or an earlier one by Shara et al. (1989); the larger cavity I report here could have originated more than 10^4 yr ago, possibly built up during successive eruptions.

4. Concluding remarks

Dust in RS Oph has been detected in between several eruptions, and at only half a year since the 2006 eruption. The silicate dust species and mass-loss rate of $\dot{M} \sim 2$ to 3×10^{-8} M$_\odot$ yr^{-1} are not at odds with the expectations for well-developed dust-driven winds of single stars. But because RS Oph has a relatively warm photosphere, weak pulsation and not very high luminosity, this might in fact suggest that the mass-loss rate *is* enhanced by the effects of the companion white dwarf. The eruptions do *not* seem to have a dramatic effect on the dust envelope. An accretion rate onto the white dwarf surface of $\dot{M} > 10^{-7}$ M$_\odot$ yr^{-1} would probably require an enhanced flow through the Lagrangian point L$_1$.

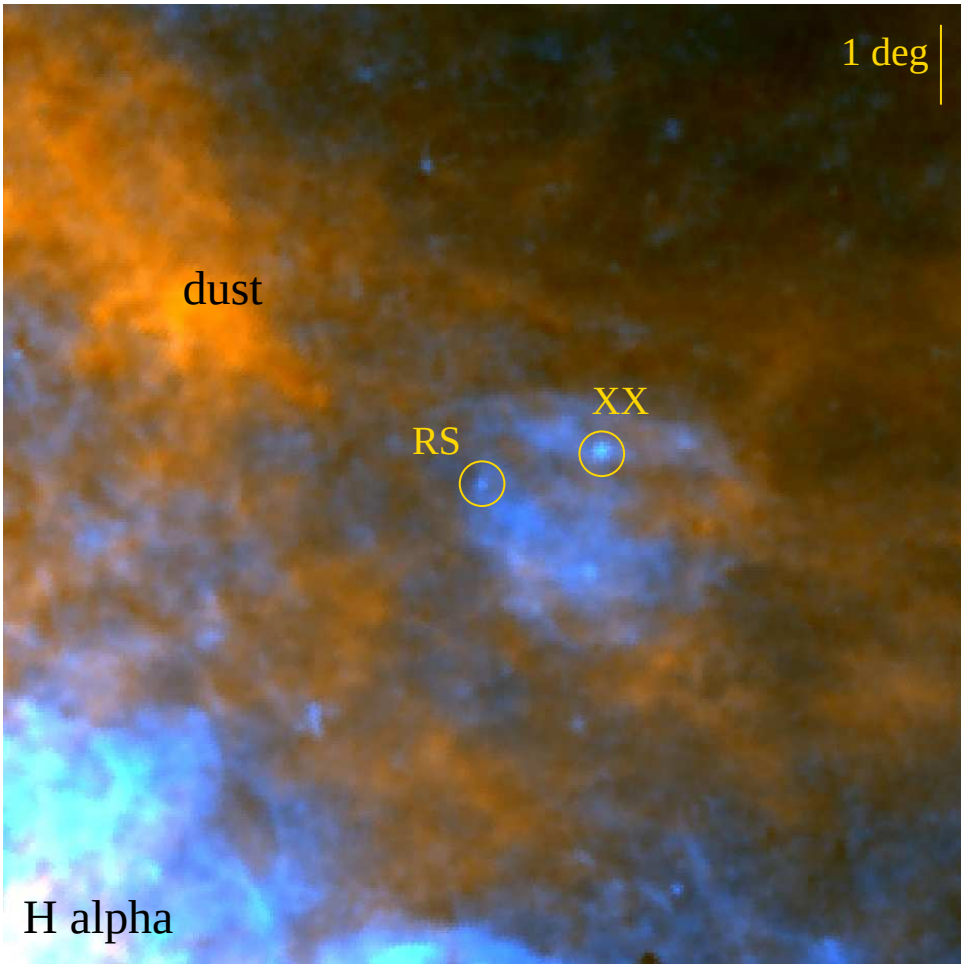

Figure 8. Combination of the COBE dust map (orange) and SHASSA Hα survey (blue), showing RS Oph and the nearby symbiotic binary XX Oph.

Considering the pattern in the time intervals between historic eruptions, including the 1907 eruption (Schaefer 2004), one might heuristically expect the next eruption to be due around 2015 (Fig. 10).

Acknowledgments. I would like to thank everyone for a pleasant meeting, and Joana Oliveira for helping me, specifically with making the colour images.

References

Bowen, G. A., & Willson, L. A. 1991. ApJ, 375, L53
Cool, R. J., Howell, S. B., Peña, M., Adamson, A. J., Thompson, R. R. 2005, PASP, 117, 462
Evans, A., et al. 2007, ApJL, submitted
Fekel, F. C., Joyce, R. R., Hinkle, K. H., & Skrutskie, M. F. 2000, AJ, 119, 1375
Finkbeiner, D. P. 2003, ApJS, 146, 407
Gail, H.-P., & Sedlmayr, E. 1987, A&A, 177, 186

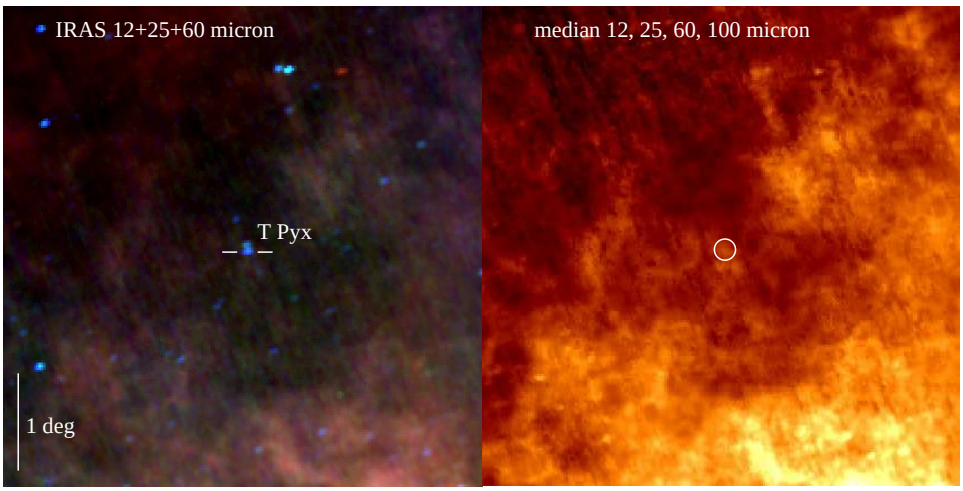

Figure 9. IRAS composites around T Pyx (North is up, East is left); the right panel is a median combination of scaled 12, 25, 60 and 100 μm images.

Geisel, S. L., Kleinmann, & D. E., Low, F. J. 1970, ApJL, 161, 101
Gilmozzi, R., & Selvelli, P. 2007, A&A, 461, 593
Girardi, L., Bressan, A., Bertelli, G., & Chiosi, C. 2000, A&AS, 141, 371
Harrison, T. E., & Gehrz, R. D. 1994, AJ, 108, 1899
Hodge, T. M., Kraemer, K. E., Price, S. D., & Walker, H. J. 2004, ApJS, 151, 299
Ivezić, Ž., & Elitzur, M. 1997, MNRAS, 287, 799
Judge, P. G., & Stencel, R. E. 1991, ApJ, 371, 357
Kenyon, S. J. 1988, AJ, 96, 337
Kenyon, S. J., Fernandez-Castro, T., & Stencel, R. E. 1986, AJ, 92, 1118
Kenyon, S. J., Fernandez-Castro, T., & Stencel, R. E. 1988, AJ, 95, 1817
Knapp, G. R. 1985, ApJ, 293, 273
Mathis, J. S., Rumpl, W., & Nordsieck, K. H. 1977, ApJ, 217, 425
McDonald, I., & van Loon, J. Th. 2007, A&A, in press (arXiv:0710.1491)
Mikołajewska, J. 2000, ASPC, 199, 431
Netzer, N., & Elitzur, M. 1993, ApJ, 410, 701
Origlia, L., Rood, R. T., Fabbri, S., Ferraro, F. R., Fusi Pecci, F., & Rich, R. M. 2007, ApJL, 667, 85
Ossenkopf, V., Henning, Th., & Mathis, J. S. 1992, A&A, 261, 567
Schaefer, B. E. 1986, PASP, 98, 556
Schaefer, B. E. 2004, IAUC, 8396, 2
Schlegel, D. J., Finkbeiner, D. P., Davis, M. 1998, ApJ, 500, 525
Shara, M. M., Moffat, A. F. J., Williams, R. E., Cohen, J. G. 1989, ApJ, 337, 720
van Loon, J. Th., Groenewegen, M. A. T., de Koter, A., Trams, N. R., Waters, L. B. F. M., Zijlstra, A. A., Whitelock, P. A., & Loup, C. 1999, A&A, 351, 559
van Loon, J. Th., Cioni, M.-R. L., Zijlstra, A. A., & loup, C. 2005, A&A, 438, 273
van Loon, J. Th., McDonald, I., Oliveira, J. M., Evans, A., Boyer, M. L., Gehrz, R. D., Polomski, E., & Woodward, C. E. 2006, A&A, 450, 339

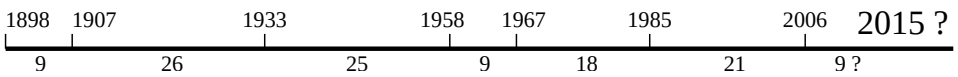

Figure 10. Recent outbursts of RS Oph and a heuristic prediction for the next.